

Design and Analysis of a Compact Reconfigurable Dual Band Notched UWB Antenna

Ponnada Mayuri¹, Nagumalli D. Rani¹,
Nemani B. Subrahmanyam¹, and Boddapati T. P. Madhav^{2, *}

Abstract—In this paper, a dual notch Ultra Wideband (UWB) monopole antenna with compact dimensions of $37.8 \times 27.1 \times 1.6 \text{ mm}^3$ is presented. Octagon patch with a defected ground structure is used to attain the wide frequency range of 3.17 GHz–11.61 GHz with ultra-wide impedance bandwidth of 8.33 GHz. The band notch characteristics in WiMAX (3.2 GHz–3.67 GHz) and WLAN (4.32 GHz–5.81 GHz) bands are achieved using inverted pi-slot in the radiating element and a pair of double split ring resonators (DSRRs) on either sides of the feed, respectively. Reconfigurability in the bands is obtained by using BAR64-03W pin diodes switching at the appropriate placement in the antenna structure. The proposed antenna exhibits efficiency of 88% in operating and 20% in non-operating frequencies. The proposed antenna is designed, simulated, and optimized using HFSS 19 electromagnetic tool. The measured results are tested using combinational analyzer in a chamber with antenna measurement setup for validation and found in good matching with simulation.

1. INTRODUCTION

Antenna plays a major role in a communication system in terms of transmission and reception of electromagnetic signals. Day-by-day, the size of electronic devices is getting reduced which insists on the need for the compact antenna. Moreover, to address several wireless services scattered over a wide frequency range, multiband antennas are required. Multiband antenna has poor isolation and leads to the occurrence of interference when multiple radios are operating simultaneously. The poor out-of-band rejection capability [1] and fixed configuration of a multiband antenna are no longer suitable for the emerging needs of today's communication system [2]. Making antennas reconfigurable can accommodate them to new operating scenarios. A reconfigurable antenna has good out-of-band rejection capability and dynamic behavior among frequency, polarization, and radiation pattern. Reconfigurability in an antenna replaces several single function antennas, and it further reduces the cost and space requirement. Reconfigurability in an antenna can be achieved through various techniques, viz., mechanically movable parts, phase shifters, attenuators, PIN diodes, and tunable materials. Reconfigurable antennas find applications in various fields [3]. Federal communications commission (FCC) declared the frequency range from 3.1 to 10.6 GHz as unlicensed, termed as UWB, in 2002 [4]. Since then, UWB communication system has become the focus of interest because of its wide band characteristics, high data rates, low power transmission, and low profile.

UWB system faces interference with narrowband wireless standards such as worldwide interoperability for microwave access (3.3 GHz–3.7 GHz) and wireless local area network (5.15 GHz to 5.85 GHz). Thus the design of a compact UWB antenna with filtering characteristics in undesired bands is a demanding criterion. However, the fixed configuration of band notch functionality limits

Received 29 August 2019, Accepted 15 December 2019, Scheduled 1 January 2020

* Corresponding author: Boddapati Taraka Phani Madhav (btpmadhav@kluniversity.in).

¹ Department of ECE, Gayatri Vidya Parishad College of Engineering (Autonomous) Visakhapatnam, India. ² Antennas and Liquid Crystals Research Center, Department of ECE, Koneru Lakshmaiah Education Foundation, Vaddeswaram, AP, India.

the antenna performance. To increase efficient utilization of the designed antenna, reconfigurability in band notches is required. Different types of structures are used to attain band notch characteristics. In [5], u-slot, meander line, and spur line structures are used to obtain the triple band reject filter. Split Ring Resonators (SRRs) as band reject structures and its different characteristics are discussed in [6, 7]. The advantages of Defected Ground Structures (DGS) and filter characteristics of different DGSs, viz., dumbbell, u-slot, v-slot, fractal DGS, and spiral DGS, are covered in [8]. U-slot in feed and H-slot in radiating patch [9, 10] cause band rejection characteristics. A Sierpinski fractal based UWB antenna is discussed in [11]. C-shaped slots and Single Split Ring Resonators (SSRR) are used to achieve band notch characteristics. A Minkowski fractal structure [12] is used to attain the band notch at WiMAX band. Split phi shape square ring (SPSSR) and split phi shape circular ring (SPSCR) antennas [13] are used for band notch applications. The incorporation of PIN diodes causes downshift in resonant frequency and reduces gain of the antenna [14, 15]. Dual-notch characteristics using a single structure is discussed in [16]. Different types of stubs [17, 18], open loop ring resonator & hair pin band stop filter [19] are used to obtain band notch characteristics. A switchable single/double notch reconfigurable antenna is designed by Badamchi et al. [20] for UWB applications.

In this paper, notch characteristics at WiMAX and WLAN bands are obtained by using an inverted pi-slot in the radiating patch and a pair of double split ring resonators (DSRR) on either sides of the feed, respectively. Section 2 includes a step by step procedure for the design of proposed antenna, viz., design of a UWB monopole antenna, employing band notch structures, and achieving reconfigurability using BAR64-03W pin diode switching technique. The performance analysis of the proposed antenna is examined using HFSS simulation, and the measurement is done for validation.

2. ANTENNA DESIGN

The proposed antenna with substrate dimensions of $37.8 \times 27.1 \times 1.6 \text{ mm}^3$ is designed on FR4 having parameters: dielectric constant $\epsilon_r = 4.4$, thickness (h) = 1.6 mm, and loss tangent ($\tan \delta$) = 0.02, which is shown in Figure 1, and the dimensions are listed in Table 1.

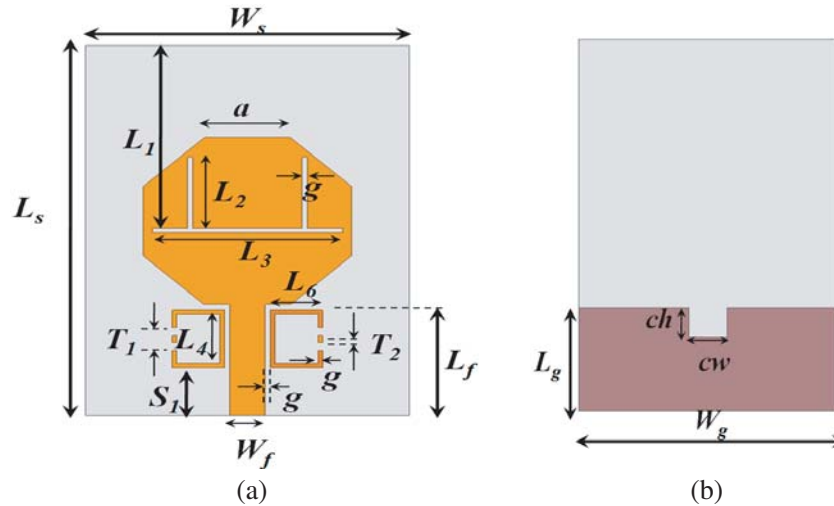


Figure 1. Dual notch UWB monopole antenna. (a) Front view. (b) Back view.

The designed UWB monopole antenna consists of an octagon-shaped structure as the radiating element to get wide band operational bandwidth. Besides that, a rectangular cut with the partial ground is used to provide impedance matching over a wide range of frequencies [21]. The antenna is designed to operate in UWB i.e., 3.1 GHz–10.6 GHz with band rejection (notch) characteristics at WiMAX (3.3 GHz–3.7 GHz) and WLAN (5.15 GHz–5.85 GHz) bands.

The step by step implementation of the dual-notch UWB monopole antenna is shown in Figure 2.

Table 1. Dimensions of Reconfigurable dual notch UWB monopole antenna.

Parameter	Value (mm)	Parameter	Value (mm)	Parameter	Value (mm)
L_s	38.7	a	7.25	L_4	6
W_s	27.1	g	0.4	L_5	4.4
L_g	10.7	ch	3	T_1	2.4
W_g	27.1	L_1	19.15	T_2	0.7
L_f	11.6	L_2	7.5	S_1	5
W_f	3.01	L_3	16	cw	4

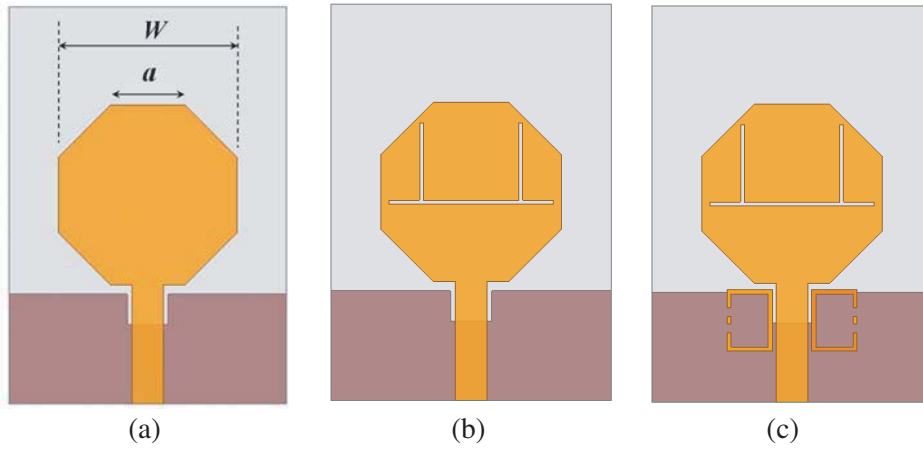


Figure 2. Step by step implementation of dual notch UWB monopole antenna. (a) UWB monopole antenna. (b) UWB monopole antenna with an inverted pi slot in the radiating element. (c) UWB monopole antenna with a pair of DSRs beside the feed.

Antenna 1 configuration is obtained by considering the square patch with side ‘ W ’ as [22]

$$W = \frac{c}{2f_r} \sqrt{\frac{2}{\epsilon_r + 1}} \tag{1}$$

where c is the speed of light $= 3 \times 10^8$ m/sec, and f_r is the operating frequency. To form the octagon shape, the corners of the square patch are truncated in such a way that side of the octagon ‘ a ’ = 7.25 mm. The width of the feed ‘ W_f ’ is given by

$$\frac{Wf}{h} = \begin{cases} \frac{8e^A}{e^{2A} - 2} & \frac{Wf}{h} \leq 2 \\ \frac{2}{\pi} \left\{ B - 1 - \ln(2B - 1) + \frac{\epsilon_r - 1}{2\epsilon_r} \left[\ln(B - 1) + 0.39 - \frac{0.61}{\epsilon_r} \right] \right\} & \frac{Wf}{h} \geq 2 \end{cases} \tag{2}$$

where $A = \frac{2\pi Z_0}{\eta} \sqrt{\frac{\epsilon_r + 1}{2}} + \frac{\epsilon_r - 1}{\epsilon_r + 1} (0.23 + \frac{0.11}{\epsilon_r})$; $B = \frac{\eta}{2Z_0 \sqrt{\epsilon_r}}$, \square = free space impedance (377 ohms).

The approximate length of the notch structure is given by

$$L_{notch} = \frac{c}{2f_{notch} \sqrt{\epsilon_{reff}}} \tag{3}$$

where c is the speed of light $= 3 \times 10^8$ m/sec, f_{notch} the center frequency of notch band, and ϵ_{reff} the effective dielectric constant ϵ_{reff} .

$$\epsilon_{reff} = \frac{\epsilon_r + 1}{2} + \frac{\epsilon_r - 1}{2} \left[1 + 12 \frac{h}{W} \right]^{-1/2}$$

The length of inverted pi-slot L_{inv} and the length of DSRR L_{DSRR} corresponding to 3.5 GHz and 5.5 GHz are calculated using Equation (3). The length of the segments in notch structures can be calculated as

$$2L_2 + L_3 = L_{inv} \quad (4)$$

$$2L_4 + L_5 - 4g - T_1 + T_2 = L_{DSRR} \quad (5)$$

The reflection coefficient characteristics of three antenna configurations are shown in Figure 3. From Figure 3, it is observed that Antenna 1 operates in the entire UWB range (3.17 GHz–11.61 GHz). Antenna 2 exhibits a notch at WiMAX (3.32 GHz–3.92 GHz) band, and Antenna 3 exhibits the notch at WLAN (5.42 GHz–6.00 GHz) band.

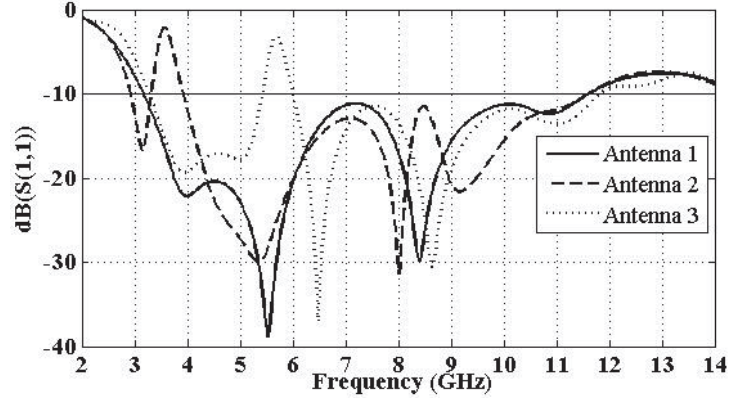


Figure 3. Reflection coefficient characteristics of Antenna 1, Antenna 2 and Antenna 3.

To bring frequency reconfigurability between the notch bands in the antenna configuration (Figure 1), BAR64-03W pin diodes are employed. The equivalent circuit model of PIN diode at high frequencies is shown in Figure 4.

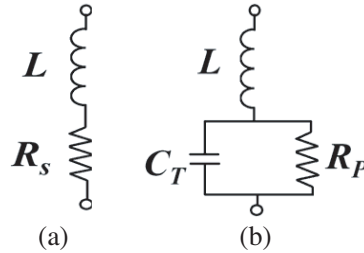


Figure 4. PIN diode equivalent circuit model. (a) ON state. (b) OFF state.

The forward resistance (R_S) of the PIN diode in ON state is 2.1Ω , and the reverse parallel resistance (R_P) and diode capacitance (C_T) in OFF state are $3.1 \text{ k}\Omega$ and 0.02 pF , respectively. The values of packaging inductance are the same for both cases, and the value is $L = 0.6 \text{ nH}$.

The proposed reconfigurable dual-notch UWB monopole antenna is shown in Figure 5 and has the same dimensions as in Table 1. The placement of the PIN diodes D_1 and D_2 across horizontal slot of the inverted-pi shaped slot in the radiating element will cause the shorting of diodes due to that infrastructure on the patch as shown in Figure 1. In order to overcome this effect, the horizontal segment of inverted-pi slot is extended further so as to provide isolation between the anode and cathode terminals of the PIN diodes D_1 and D_2 which are incorporated. This will not create any hindrance for biasing of diodes.

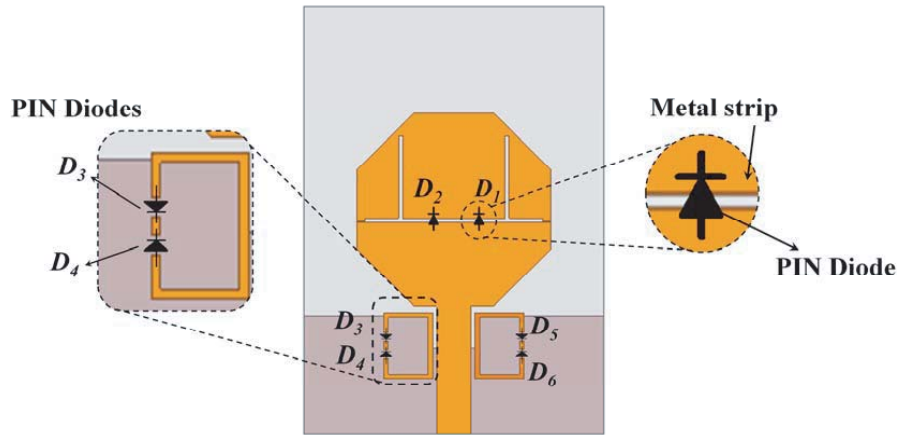


Figure 5. Reconfigurable dual notch UWB monopole antenna.

3. RESULTS AND DISCUSSION

3.1. Significance of DSRR

The geometry of UWB monopole antenna with a Single Split Ring Resonator (SSRR) and Double Split Ring Resonator (DSRR) is shown in Figure 6, and the dimensions are the same as in Table 1.

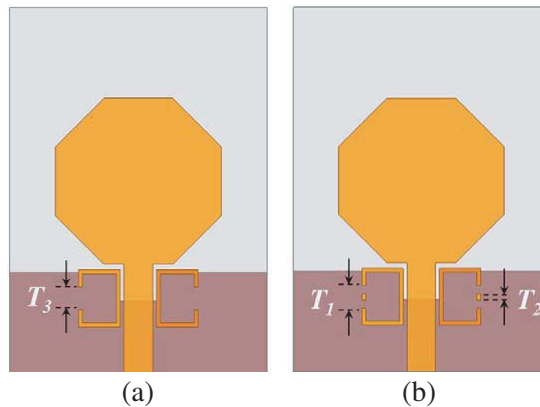


Figure 6. UWB monopole antenna with (a) SSRR having gap $T_3 = 2$ mm, (b) DSRR having $T_1 = 2.4$ mm and $T_2 = 0.7$ mm.

The reflection coefficient characteristics of UWB monopole antenna with SSRR and DSRR are shown in Figure 7.

From Figure 7, it is observed that SSRR exhibits a notch at 5.19 GHz–5.80 GHz, whereas DSRR exhibits notch characteristics at 5.42 GHz–6.00 GHz. The additional gap in the DSRR causes a reduction in equivalent capacitance and leads to the shift in frequency as compared to SSRR.

The PIN diode loaded SSRR and DSRR structures are shown in Figure 8.

The configuration of SSRR is not suitable for switching operation. The diode placement in SSRR causes the short circuit of diode terminals as shown in Figure 8(a). This leads to the improper functioning of the diode. To avoid this problem, DSRR structures are used. The diodes are placed back to back in DSRR as shown in Figure 8(b).

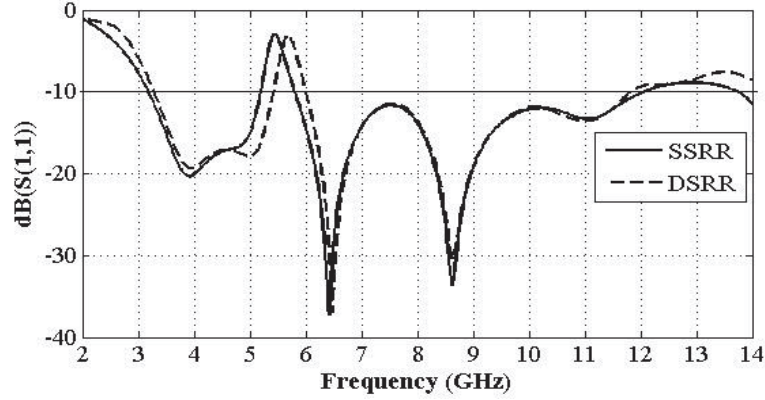


Figure 7. Reflection coefficient characteristics of UWB monopole antenna with SSRR and DSRR.

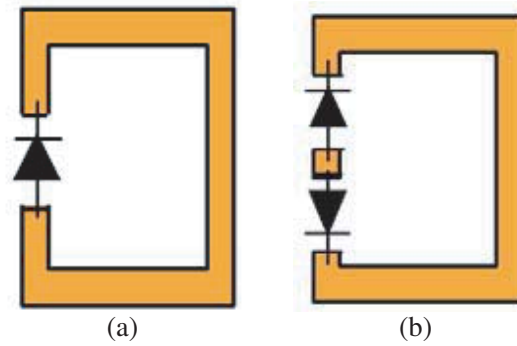


Figure 8. Diode representation in (a) SSRR, (b) DSRR.

3.2. Current Distribution

The current distribution of dual-notch UWB monopole antenna without PIN diodes is shown in Figure 9.

From Figure 9, it is observed that there is no radiation at notch band frequencies. This causes a reduction in gain and efficiency at notch band frequencies. The gain and efficiency plots of dual-notch UWB monopole antenna are shown in Figure 10.

From Figure 10, it is observed that the gain variation is within 3.5 dB except at the notch band frequencies. A significant gain reduction is observed at the notch band frequencies. The efficiencies of the proposed antenna are 88% and 20% at operating and notch band frequencies, respectively.

The measured radiation patterns of the proposed antenna at 3.5 GHz, 4.5 GHz, 5.5 GHz, and 7 GHz including E -plane and H -plane are shown in Figure 11.

From Figure 11, it is observed that the proposed antenna exhibits omnidirectional pattern in H -plane and dipole like pattern in E -plane. Polynomial factorization plus linear programming optimization based effective approaches can be used in element excitation to improve the beam pattern [23].

3.3. Measured Results

The proposed reconfigurable dual-notch UWB monopole antenna is fabricated using a PCB prototype machine Nvis 72 and tested using Anritsu Vector Network Analyzer (VNA). The prototype of fabricated design and its test setup is shown in Figure 12.

The fabricated antenna is fed through an SMA coaxial cable of VNA. A DC block (MCL 15542 BLK-89-S+) is used in between the SMA connector of the antenna and VNA cable to eliminate the adverse effects of DC current with the RF current paths and to protect measuring instrument by blocking the DC current towards the input port of measuring instrument. The proposed reconfigurable UWB monopole antenna can operate in four states as shown in Table 2.

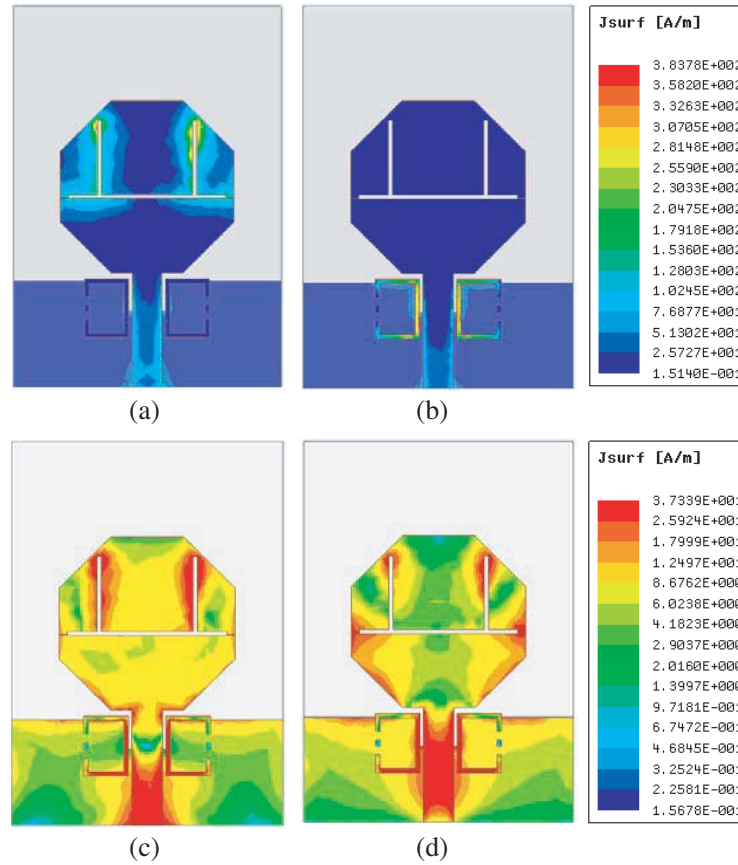


Figure 9. Current distribution of antenna at notch and operating bands. (a) 3.5 GHz, (b) 5.5 GHz, (c) 4.5 GHz, (d) 7 GHz.

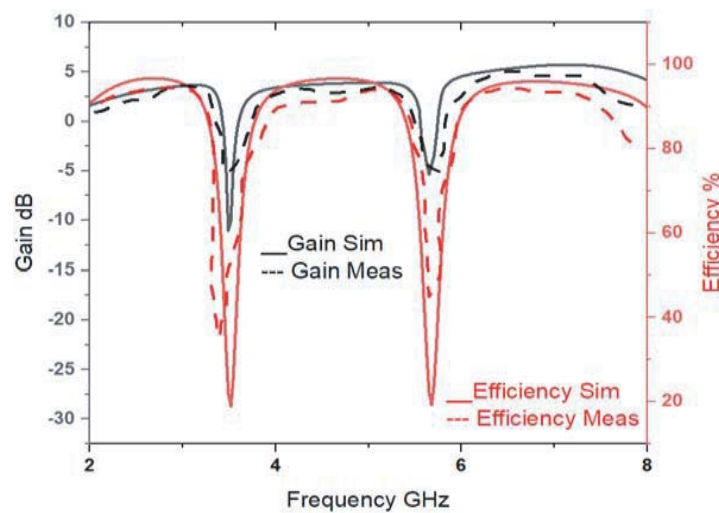


Figure 10. Gain and efficiency plots of dual-notch UWB monopole antenna without PIN diodes.

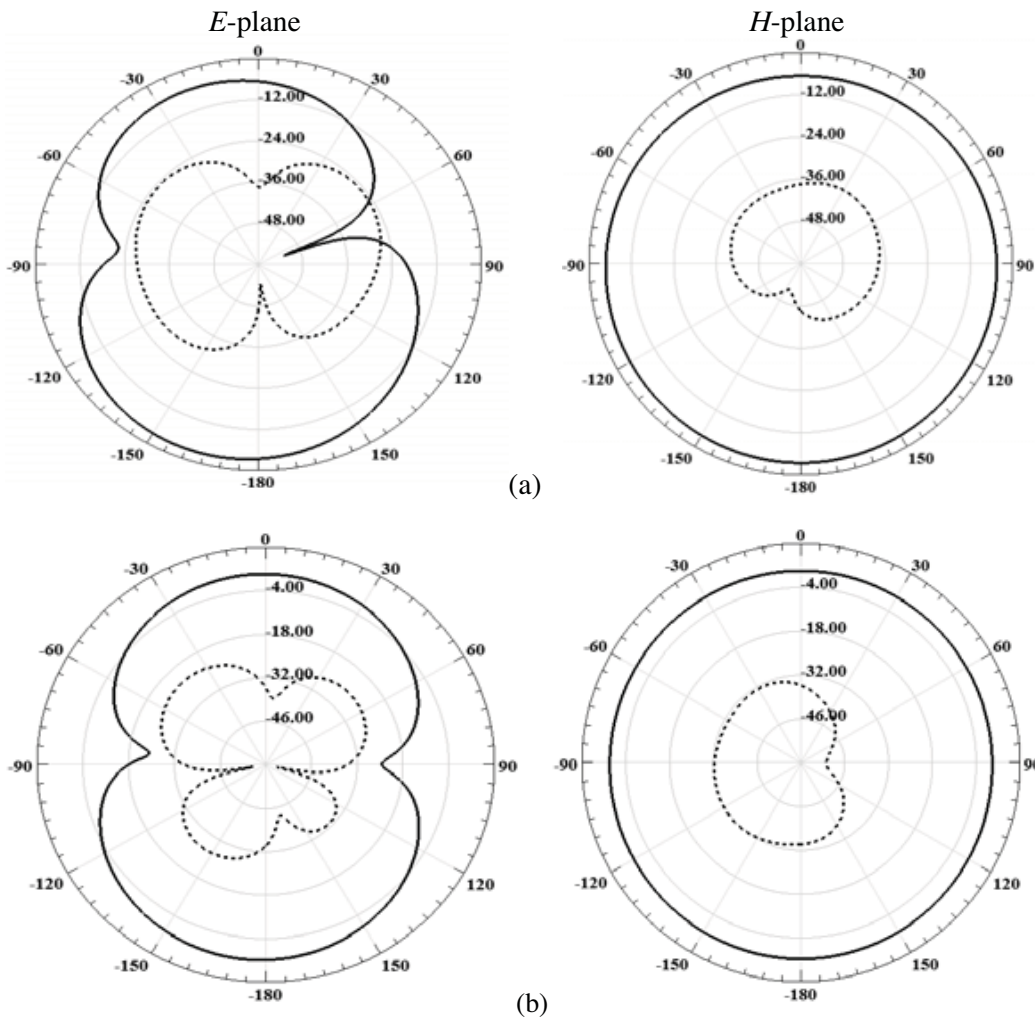
When all the diodes are in ON condition (i.e., State-4), the proposed antenna operates in the UWB range. The reflection coefficient characteristics in state-1 to state-4 are shown in Figure 13 to Figure 16. The four states provide four conditions with respect to the notching. State 1 provides dual notches at desired bands, and state 2 provides notching at WiMAX. State 3 provides a notch at WLAN band,

Table 2. Operating states of the proposed antenna.

State	D1 & D2	D3, D4, D5 & D6	Notch bands
1	OFF	OFF	WiMAX & WLAN
2	OFF	ON	WiMAX
3	ON	OFF	WLAN
4	ON	ON	—

Table 3. Comparison of simulated and measured results of the proposed antenna.

State	Frequency (GHz)	
	Simulated	Measured
1	3.29 GHz–3.89 GHz & 5.13 GHz–5.65 GHz	3.20 GHz–3.67 GHz & 4.32 GHz–5.81 GHz
2	3.22 GHz–3.92 GHz	3.32 GHz–3.55 GHz
3	5.16 GHz–5.72 GHz	5.46 GHz–6.51 GHz
4	3.18 GHz–11.72 GHz	3.18 GHz–12.2 GHz



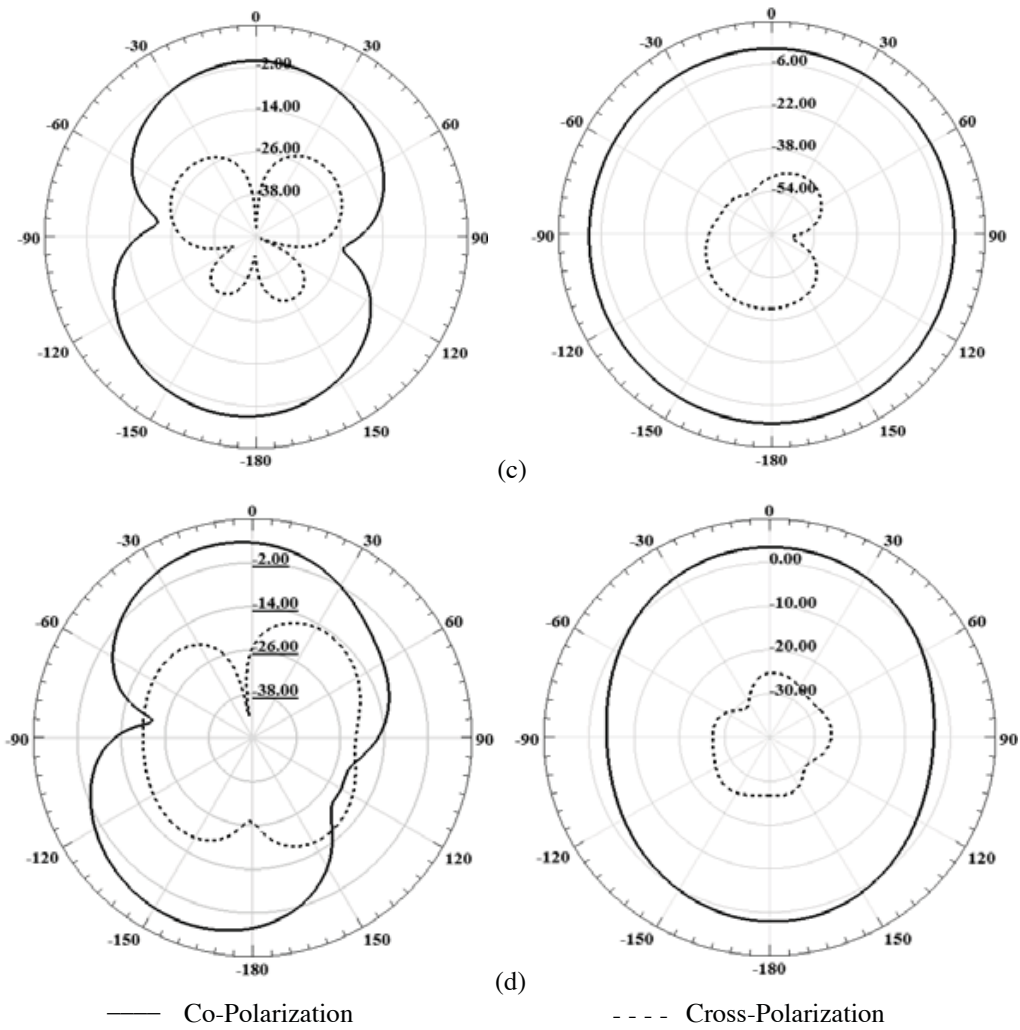


Figure 11. Radiation patterns at (a) 3.5 GHz, (b) 4.5 GHz, (c) 5.5 GHz, (d) 7 GHz.

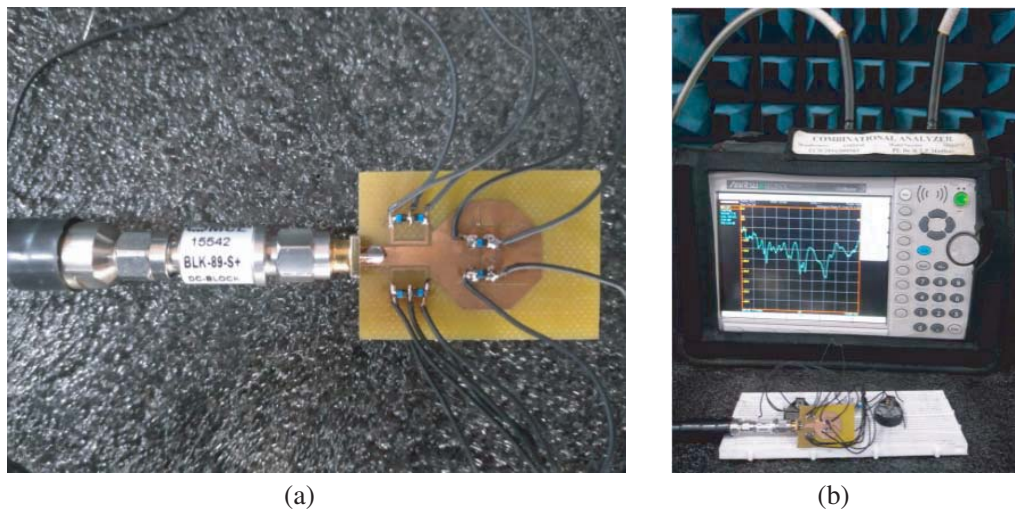


Figure 12. Reconfigurable dual notch UWB monopole antenna. (a) Fabricated design with SMA DC block. (b) Test setup using VNA.

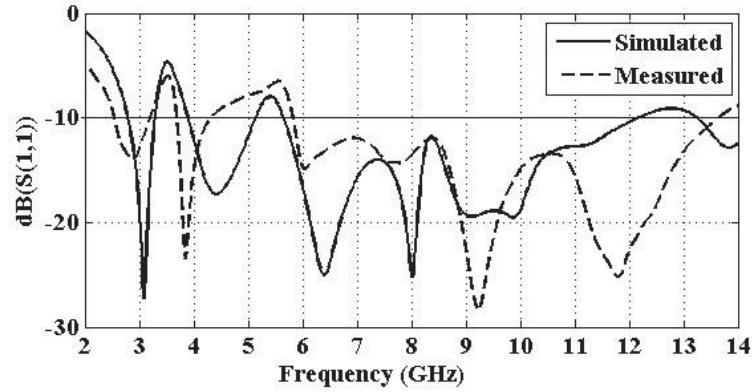


Figure 13. Reflection coefficient characteristics in state-1.

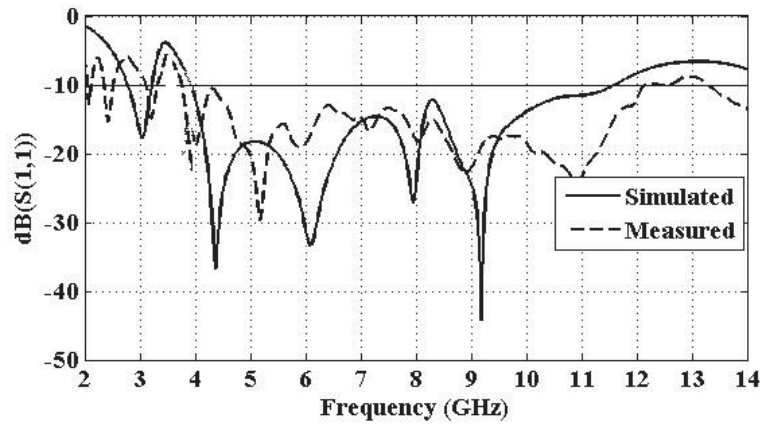


Figure 14. Reflection coefficient characteristics in state-2.

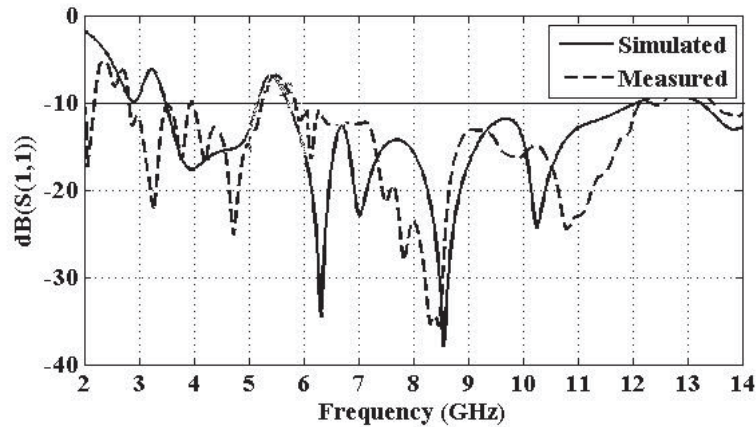


Figure 15. Reflection coefficient characteristics in state-3.

and state 4 is a wideband antenna. This reconfigurable antenna provides multiple options to the operator to utilize the antenna in four different conditions effectively. The simulated and measured frequencies of four states are listed in Table 3.

The performance of proposed antenna in comparison to the existed designs is described in Table 4. From Table 4, it is seen that the proposed antenna offers smaller size than the existing antenna

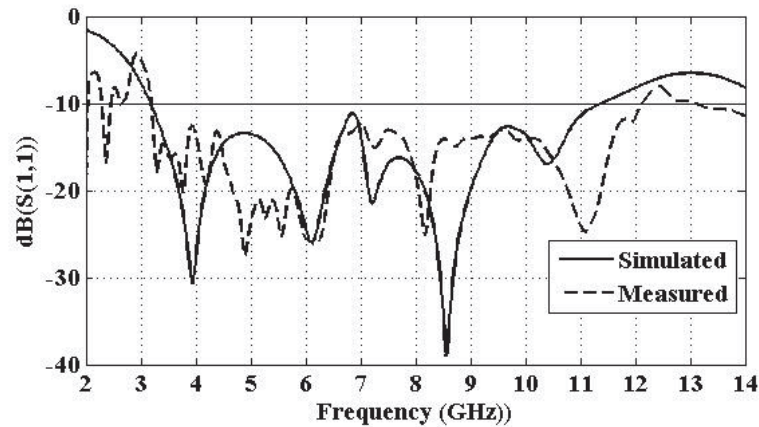


Figure 16. Reflection coefficient characteristics in state-4.

Table 4. Comparison of proposed work with existed works.

Ref.	Substrate size (mm ³)	Notching structure	Notch band (GHz)	Reconfigurability
[7]	40 × 35 × 1.5	Complementary Split ring resonators	3.3–3.7 5.15–5.35	Yes
[9]	40 × 30 × 0.787	U-slot	5.1–5.8	Yes
[10]	35 × 30 × 1.6	H & U-slots	5.15–5.85 7.25–7.75	No
[12]	26 × 16.5 × 1.6	Minkowski fractal & single SRR	3.4–3.7 5.15–5.825	No
[13]	72 × 23 × 1.6	Split phi shape square & circular rings	5.1–6.29 4.94–5.91	No
[16]	12 × 18 × 1.6	I and rotated T-shaped conductors	5–6 7.25–7.75	No
[17]	34 × 27 × 0.787	Rectangular strip and U-shaped strip	2.975–4.75 4.975–6.625	Yes
[18]	40 × 30 × 1	N & Q-shaped stubs	3.27–3.83 4.60–5.90	No
[19]	40 × 38 × 1.6	Open loop resonator & hair pin band stop filter	2.4 5.8	Yes
This work	38.7 × 27.1 × 1.6	Inverted pi-slot and double SRR	3.20–3.67 4.32–5.81	Yes

designs. In addition to that, the performance of diode loaded DSRR is discussed in this work. Although [10, 12, 16] provide smaller size, they are fixed in configuration. Even though [17] has smaller size and reconfigurability behavior, the cost is high compared to the proposed antenna design.

4. CONCLUSION

A compact UWB antenna with reconfigurable band notch characteristics at WiMAX and WLAN bands is presented. The band notch characteristics at WiMAX and WLAN bands are obtained by placing an inverted pi-slot in the radiating patch and a pair of double split ring resonators (DSRRs) on either sides of the feed, respectively. BAR64-03W PIN diodes are employed to achieve the reconfigurability between the frequency bands. The advantage of the proposed antenna is that the single antenna structure with substrate dimensions of $37.8 \times 27.1 \times 1.6 \text{ mm}^3$ provides the UWB range (3.18 GHz–12.2 GHz) as well as reconfigurable band notch characteristics. The gain variation of the proposed antenna is within 3.5 dB except at notch bands. A significant gain reduction is observed at notch band frequencies. The proposed antenna has efficiency of 88% in operating and 20% in non-operating frequencies. The performance of the proposed antenna can be further improved using Defected Ground Structures (DGSs).

REFERENCES

1. Yang, S., C. Zhang, H. K. Pan, A. E. Fathy, and V. K. Nair, "Frequency-reconfigurable antennas for multiradio wireless platforms," *IEEE Microwave Magazine*, Vol. 10, No. 1, 66–83, Feb. 2009.
2. Costantine, J., Y. Tawk, S. E. Barbin, and C. G. Christodoulou, "Reconfigurable antennas: Design and applications," *Proceedings of the IEEE*, Vol. 103, No. 3, 424–437, Mar. 2015.
3. Christodoulou, C. G., Y. Tawk, S. A. Lane, and S. R. Erwin, "Reconfigurable antennas for wireless and space applications," *Proceedings of the IEEE*, Vol. 100, No. 7, 2250–2261, Jul. 2012.
4. Di Benedetto, M.-G., T. Kaiser, A. F. Molish, I. Oppermann, C. Politano, and D. Porcino, *UWB Communication Systems: A Comprehensive Overview*, Hindawi Publishing Corporation, 2006.
5. Li, Y., S. Luo, and W. Yu, "A compact tunable triple stop-band filter based on different defected microstrip structures," *Applied Computational Electromagnetics Society Journal*, Vol. 33, No. 7, Jul. 2018.
6. Öznazi, V. and V. B. Ertürk, "A comparative investigation of SRR and CSRR based band reject filters: Simulations, experiments, and discussions," *Microw. Opt. Technol. Lett.*, Vol. 50, No. 2, 519–523, Feb. 2008.
7. Zhao, D., L. Lan, Y. Han, F. Liang, Q. Zhang, and B.-Z. Wang, "Optically controlled reconfigurable band notched UWB antenna for cognitive radio applications," *IEEE Photonics Technology Letters*, Vol. 26, No. 21, 1502–1504, Nov. 1, 2014.
8. Khandelwal, M. K., B. K. Kanaujia, and S. Kumar, "Defected ground structure: Fundamentals, analysis, and applications in modern wireless trends," *International Journal of Antennas and Propagation*, Vol. 1, 1–22, 2017.
9. Alhegazi, A., Z. Zakaria, N. A. Shairi, A. Salleh, and S. Ahmed, "Compact UWB filtering-antenna with controllable WLAN band rejection using defected microstrip structure," *Radio Engineering*, Vol. 27, 110–117, 2018.
10. Awad, N. and M. Abdelazeez, "Multislot microstrip antenna for ultra-wide band applications," *Journal of King Saud University — Engineering Sciences*, Vol. 30, No. 1, 38–45, 2015.
11. Tripathi, S., A. Mohan, and S. Yadav, "A compact fractal UWB antenna with reconfigurable band notch functions," *Microw. Opt. Technol. Lett.*, Vol. 58, No. 3, 509–514, Mar. 2016.
12. Tripathi, S., A. Mohan, and S. Yadav, "A compact UWB antenna with dual 3.5/5.5 GHz band-notched characteristics," *Microw. Opt. Technol. Lett.*, Vol. 57, No. 3, 551–556, 2015.
13. Ajetrao, K. V. and A. P. Dhande, "Phi shape UWB antenna with band notch characteristics," *Engineering, Technology & Applied Science Research*, Vol. 8, No. 4, 3121–3125, 2018.
14. Shirazi, M., J. Huang, T. Li, and X. Gong, "A switchable-frequency slot-ring antenna element for designing a reconfigurable array," *IEEE Antennas and Wireless Propagation Letters*, Vol. 17, No. 2, 229–233, Feb. 2018.
15. Shirazi, M., T. Li, and X. Gong, "Effects of PIN diode switches on the performance of the reconfigurable slot-ring antenna," *IEEE 16th Annual Wireless and Microwave Technology Conference (WAMICON)*, 3, Cocoa Beach, FL, 2015.

16. Ojaroudi, Y., S. Ojaroudi Parchin, and N. Ojaroudi Parchin, "A novel 5.5/7.5 GHz dual band-stop antenna with modified ground plane for UWB communications," *Wireless Personal Communications*, Vol. 81, 319–332, 2014.
17. Tang, M. C., H. Wang, T. Deng, and R. W. Ziolkowski, "Compact planar ultra-wideband antennas with continuously tunable, independent band-notched filters," *IEEE Transactions on Antennas and Propagation*, Vol. 64, No. 8, 3292–3301, 2016.
18. Lin, Y., J. Liang, G. Wu, Z. Xu, and X. Niu, "A novel UWB antenna with dual band notched characteristics," *Frequenz*, Vol. 69, No. 11–12, 479–483, 2015.
19. Deng, J., S. Hou, L. Zhao, and L. Guo, "A reconfigurable filtering antenna with integrated bandpass filters for UWB/WLAN applications," *IEEE Transactions on Antennas and Propagation*, Vol. 66, No. 1, 401–404, Jan. 2018.
20. Badamchi, B., J. Nourinia, C. Ghobadi, and A. V. Shahmirzadi, "Design of compact reconfigurable ultra-wideband slot antenna with switchable single/dual band notch functions," *IET Microwaves, Antennas & Propagation*, Vol. 8, No. 8, 541–548, Jun. 4, 2014.
21. Tasouji, N., J. Nourinia, C. Ghobadi, and F. Tofigh, "A novel printed UWB slot antenna with reconfigurable band-notch characteristics," *IEEE Antennas and Wireless Propagation Letters*, Vol. 12, 922–925, 2013.
22. Balanis, C. A., *Antenna Theory: Analysis and Design*, 2016.
23. Isernia, T. and A. F. Morabito, "Mask-constrained power synthesis of linear arrays with even excitations," *IEEE Transactions on Antennas and Propagation*, Vol. 64, No. 7, 3212–3217, 2016.